TGFβ superfamily signals are required for morphogenesis of the kidney mesenchyme progenitor population

Leif Oxburgh[1], Gerald C. Chu[1,2], Simon K. Michael[3] and Elizabeth J. Robertson[1,*]

[1]Department of Molecular and Cellular Biology, Harvard University, 16 Divinity Avenue, Cambridge, MA 02138, USA
[2]Department of Pathology, Brigham and Women's Hospital, 75 Francis Street, Boston, MA 02115, USA
[3]Department of Pediatrics, Tufts-New England Medical Center, 750 Washington Street, Boston, MA 02111, USA
*Author for correspondence (e-mail: Elizabeth.Robertson@well.ox.ac.uk)

Accepted 23 June 2004

Development 131, 4593-4605
Published by The Company of Biologists 2004
doi:10.1242/dev.01324

Summary

The TGFβ superfamily plays diverse and essential roles in kidney development. *Gdf11* and *Bmp4* are essential for outgrowth and positioning of the ureteric bud, the inducer of metanephric mesenchyme. During nephrogenesis, *Bmp7* is required for renewal of the mesenchyme progenitor population. Additionally, in vitro studies demonstrate inhibitory effects of BMPs and TGFβs on collecting duct branching and growth. Here, we explore the predicted models of TGFβ superfamily function by cell-specific inactivation of *Smad4*, a key mediator of TGFβ signaling. Using a *HoxB7cre* transgene expressed in ureteric bud and collecting duct, we find that development of the collecting duct is Smad4 independent. By contrast, removal of *Smad4* in nephrogenic mesenchyme using the *Bmp7*$^{cre/+}$ allele leads to disorganization of the nephrogenic mesenchyme and impairment of mesenchyme induction. *Smad4*-deficient metanephric mesenchyme does not display defects in inducibility in LiCl or spinal cord induction assays. However, in situ hybridization and lineage analysis of *Smad4* null mesenchyme cells at E11.5 show that the nephrogenic mesenchyme does not aggregate tightly around the ureteric bud tips, but remains loosely associated, embedded within a population of cells expressing markers of both nephrogenic mesenchyme and peripheral stroma. We conclude that the failure of recruitment of nephrogenic mesenchyme leaves a primitive population of mesenchyme at the periphery of the kidney. This population is gradually depleted, and by E16.5 the periphery is composed of cells of stromal phenotype. This study uncovers a novel role for TGFβ superfamily signaling in the recruitment and/or organization of the nephrogenic mesenchyme at early time-points of kidney development. Additionally, we present conclusive genetic lineage mapping of the collecting duct and nephrogenic mesenchyme.

Supplemental data available online

Key words: BMP, Kidney development, Lineage analysis, Nephrogenic mesenchyme, Smad4, Stroma, TGFβ

Introduction

Gene targeting studies have demonstrated that numerous organ systems are dependent on TGFβ superfamily signaling for their development. Because of the ease of culture of the metanephros (Saxén, 1987), findings from these experiments are complemented by in vitro studies of the effects of the addition of TGFβ superfamily ligands on kidney development (Dudley et al., 1999; Ritvos et al., 1995). Taken together, these results have significantly advanced our understanding of TGFβ superfamily function. Here, we explore the predicted roles of TGFβ superfamily signals in the kidney using the Cre-loxP system for cell-specific inactivation of *Smad4*, a key mediator of TGFβ signaling.

Development of the kidney

The Wolffian duct (WD) differentiates from mesoderm within the nephrogenic cord at approximately E9.0 in the mouse, and induces pro- and mesonephric tubules as it extends caudally toward the cloaca. At approximately E10.5, the ureteric bud (UB) appears as a thickening of the WD at the level of the hindlimb. The UB grows out in a cranial direction and invades the metanephric blastema, a population of cells at the caudal end of the nephrogenic cord. Upon induction by the metanephric mesenchyme, the UB extends and branches within the mesenchyme, forming the collecting duct (CD) system. In turn, metanephric mesenchyme is induced to condense and form nephrogenic mesenchyme (NM), which gives rise to the nephron. This cycle of induction initiates a program of reciprocal interactions between the mesenchyme and the CD epithelium. The molecular signals governing these processes are only partially understood: glial cell-derived neurotrophic factor (Gdnf), produced by mesenchyme, and signaling through the receptor tyrosine kinase Ret (c-ret) in CD epithelium, is required for directional growth and branching of collecting ducts (Sanchez et al., 1996; Schuchardt et al., 1994; Vega et al., 1996). The inductive signals to the mesenchyme remain unknown.

TGFβ superfamily signal transduction

The TGFβ superfamily is composed of a collection of structurally related ligands with diverse functions in development (Miyazono et al., 2001). Two distinct families of

receptors elicit diverse responses to ligand binding; TGFβ, nodal and activin result in phosphorylation of receptor-associated Smads (R-Smads) 2 and 3, whereas the BMPs elicit phosphorylation of R-Smads 1, 5 and 8. The GDF group comprises factors that signal via both R-Smads 2 and 3, and R-Smads 1, 5 and 8. Phosphorylated R-Smads associate with Smad4, which contains a nuclear translocation signal. In the nucleus, the R-Smad:Smad4 complex associates with a variety of cofactors that determine the outcome of the transcriptional response (Massagué, 2000). Smad4 is thus an integral component of the signal transduction machinery employed by both the TGFβ and BMP pathways.

The role of TGFβ superfamily signaling in metanephric kidney development

A role for *Gdf11* in induction of the metanephros has recently been shown. Mice deficient for *Gdf11* display uni- or bilateral kidney agenesis. Normally, Gdf11 from either the ureteric bud or the metanephric mesenchyme activates *Gdnf* expression in mesenchyme cells, which initiates the reciprocal inductive program leading to formation of the kidney (Esquela and Lee, 2003). *Tgfb2* has also been implicated in induction of the metanephros, as loss of *Tgfb2* gives rise to incompletely penetrant kidney agenesis in females (Sanford et al., 1997). In addition, Tgfβ2 has been identified as an active component of rat ureteric bud conditioned medium with inductive capacity (Plisov et al., 2001).

Genetic studies have shown roles for *Bmp4* and *Bmp7* in organogenesis of the kidney. Loss of *Bmp7* leads to premature termination of kidney development, with a depletion of nephrogenic mesenchyme cells (Dudley et al., 1995). Explant experiments indicate that Bmp7 acts as a survival factor for nephrogenic progenitor cells, suggesting that Bmp7 is required in vivo for replenishment of the progenitor cell pool (Dudley et al., 1999). *Bmp4* expressed in mesenchyme surrounding the Wolffian duct inhibits ectopic budding of the ureteric bud (Miyazaki et al., 2000). Additionally, in embryos that form a single ureteric bud there is a paucity of epithelial structures in the E14.5 kidney (Miyazaki et al., 2003). The reduction in nephron number and the premature arrest of kidney development indicate that Bmp4 may also act as a survival signal for nephrogenic mesenchyme.

In this study we have used cell-type specific inactivation of *Smad4* to further define the role of TGFβ superfamily signals in kidney development. Surprisingly, removal of *Smad4* in the epithelium of the Wolffian duct, the ureteric bud and the collecting duct system does not impair the development of the metanephros. However, loss of *Smad4* in the metanephric mesenchyme leads to ectopic mesenchymal cell death and premature depletion of nephrogenic mesenchyme. Strikingly, there is a marked expansion of the peripheral stromal layer and impaired condensation of nephrogenic mesenchyme, implying a role for TGFβ signaling in the morphogenesis of the mesenchyme at the earliest stages of nephrogenesis.

Materials and methods

Mouse strains

The *Bmp7*$^{cre/+}$ strain was generated by inserting an Internal Ribosomal Entry Site (IRES), *Cre* recombinase cDNA and FRT-flanked *PGK-hygromycin* cassettes (Michael et al., 1999) into coding exon 1 of the *Bmp7* gene. The targeting vector containing 3.5 kb 5′ and 4.5 kb 3′ homology arms (Godin et al., 1998) was transfected into CCE ES cells that were grown under drug selection as previously described (Michael et al., 1999). Correctly targeted clones were identified by Southern hybridization and used to generate germ line chimeras. Adults were intercrossed with mice expressing *FLP* recombinase under the control of the human *β-actin* promoter (Dymecki, 1996), and offspring were PCR-genotyped for loss of the *hygromycin* cassette.

The *HoxB7cre* transgene was generated by cloning *Cre* recombinase cDNA fused to a nuclear localization signal (Gu et al., 1993) into a cassette containing the *HoxB7* enhancer/promoter element, a polylinker and 3′ sequence from the human *β-globin* gene with a splice donor, acceptor and polyadenylation site (Srinivas et al., 1999). *Pml*I linearized DNA was microinjected into fertilized oocytes using standard procedures (Hogan et al., 1994), and offspring were genotyped by *Cre* PCR. Positive males were intercrossed with *ROSA26*^{R} reporter females (Soriano, 1999), and embryos were dissected and stained at E14.5 to verify Cre activity in the collecting duct system of the kidney. Of six positive males, two showed reliable excision in collecting ducts. Both strains were used in this study.

The Smad4 conditional strain carries loxP sites flanking the first coding exon of Smad4, which results in removal of the DNA-binding domain and nuclear localization signal upon recombination (Chu et al., 2004).

Sample preparation

For Hematoxylin and Eosin staining, in situ hybridization and immunohistochemistry, tissues were fixed in 4% paraformaldehyde in PBS, dehydrated, embedded in paraffin wax, and sectioned at 6 μm. Hematoxylin and Eosin staining was performed using standard procedures. For X-Gal staining, whole tissues were fixed for 90 minutes in 0.5% glutaraldehyde, 1% paraformaldehyde in PBS, and staining was performed as described previously (Michael et al., 1999).

In situ hybridization

Sections were rehydrated and in situ hybridization was performed using standard procedures (Mendelsohn et al., 1999). Whole mount in situ hybridization was performed as described previously (Wilkinson, 1992). Probes used in this study were: Wt1 (Kreidberg et al., 1993), Pax2 (Dressler et al., 1990), Ret (Pachnis et al., 1993), Raldh2 (Batourina et al., 2001), Lhx1 (Barnes et al., 1994) and Gdnf (Hellmich et al., 1996).

Immunohistochemistry

Immunohistochemistry was performed as described (Oxburgh and Robertson, 2002), with 1:200 dilutions of affinity-purified rabbit antisera specific for phosphorylated Smad1 and phosphorylated Smad2 (a kind gift of Peter ten Dijke). Pax2 staining with antigen unmasking was performed as described (Schnabel et al., 2001). PCNA staining was performed using the PC10 mouse monoclonal antibody (Santa Cruz Biotechnology) and the Mouse-on-Mouse kit (Vector Laboratories), according to the manufacturer's instructions.

RT-PCR assays

E11.5 kidneys and E17.5 whole embryos were dissected into Trizol (Invitrogen), and RNA was extracted according to the manufacturer's instructions. cDNA synthesis and PCR were performed as previously described (Oxburgh and Robertson, 2002). The oligonucleotide combinations used to amplify transcripts for members of the TGFβ superfamily are listed in the supplementary table (see Table S1 at http://dev.biologists.org/cgi/content/full/131/18/4593/DC1).

Kidney explant culture

Mesenchymes were separated from ureteric buds of E11.5 kidneys, as previously described (Godin et al., 1998), and cultured on filter rafts with and without 15 mM LiCl in the culture medium. After 72 hours,

cultures were either processed for sectioning, or stained for laminin as described (Bard et al., 2001) and viewed using a Zeiss LSM510 confocal microscope.

Results

To delete *Smad4* in the developing metanephros, we made use of the *Smad4* conditional allele previously described (Chu et al., 2004). Two individual Cre recombination strategies were employed. We generated transgenic mice expressing *Cre* recombinase under the control of *HoxB7* regulatory elements (Srinivas et al., 1999) in order to eliminate *Smad4* in the ureteric epithelium. In parallel, we introduced *Cre* recombinase into the endogenous *Bmp7* locus to study the effects of *Smad4* removal in mesenchyme (Fig. 1A). The extent of Cre activity of *HoxB7cre* and *Bmp7*$^{cre/+}$ was evaluated by crossing each strain with the *ROSA26*^{R} reporter, in which Cre-mediated DNA recombination activates the *lacZ* reporter (Soriano, 1999).

Cell-type-specific excision by *Bmp7*$^{cre/+}$ and *HoxB7cre* reveals lineage relationships in the metanephros

As *lacZ* expression serves as a heritable genetic marker, this enabled us to perform lineage analysis of cells derived from the ureteric bud and nephrogenic mesenchyme, in addition to selectively inactivating *Smad4* in regions of the developing kidney. The *HoxB7cre* transgene recombines completely in the ureteric bud by E11.5 (Fig. 1J), and the collecting ducts consist entirely of labeled cells through to E17.5, the last stage examined (data not shown). Cells of collecting duct origin remain strictly segregated from the distal tubule (Fig. 1K and data not shown). Occasional labeled cells can be seen at low frequency in the stroma, which we attribute to migration of *HoxB7*-expressing cells from the neural crest. We conclude that cells derived from the ureteric bud are restricted to forming the collecting duct system.

Bmp7$^{cre/+}$ activated the *ROSA26*^{R} reporter in components of the kidney derived from both the ureteric bud and the metanephric mesenchyme. From the earliest stages of metanephric development, recombination occurs in the ureteric bud, and subsequently labeled cells are seen throughout the collecting duct system. At E11.5, there is mosaic recombination throughout the metanephric mesenchyme (Fig. 1B), and by E12.0, labeling is evident within the four to five cell layers of nephrogenic mesenchyme around collecting duct tips, with a few unlabeled cells surrounding collecting duct trunks and the periphery of the kidney (Fig. 1C). At E13.5, labeled cells are seen in nephrogenic mesenchyme and epithelial structures such as renal vesicles, comma-shaped bodies, Bowman's capsule and podocytes (Fig. 1D,F,G). Interestingly, labeling is not seen in the peripheral stroma. The medullary stroma contains a few labeled cells, which we attribute to migration of *Bmp7*-expressing cells of neural origin. This general pattern of labeling is maintained up to E17.5 (data not shown).

We next compared *Bmp7*$^{lacZ/+}$ reporter expression (Godin et al., 1998) with the domain of *Rosa26*^{R} activation by *Bmp7*$^{cre/+}$. *Bmp7*$^{lacZ/+}$ is expressed throughout the collecting ducts, but is restricted in the mesenchyme (Fig. 1E). Expression is robust in nephrogenic mesenchyme, but is maintained in only a few

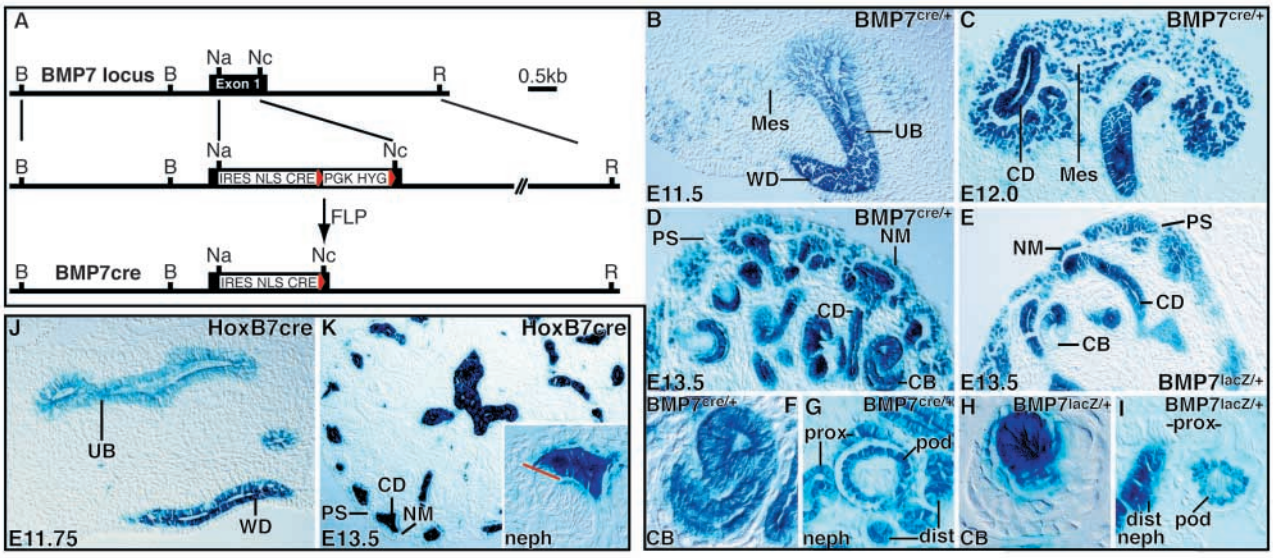

Fig. 1. Generation and characterization of the *Bmp7*$^{cre/+}$ and *HoxB7cre* kidney deleter strains. (A) Targeting strategy used to generate *Bmp7*$^{cre/+}$. (B,C,D) *Bmp7*$^{cre/+}$ activates the *ROSA26*^{R} reporter in Wolffian duct, ureteric bud and the collecting duct system. Mesenchyme excision is scattered through the metanephric blastema at E11.5 (B), and by E12.0 (C), is uniform throughout the mesenchyme condensates surrounding collecting duct tips. A population of cells surrounding the collecting duct trunk is devoid of excision at this stage. At E13.5 (D), excision is limited to the collecting ducts, nephrogenic mesenchyme, renal vesicles, comma- and s-shaped bodies and podocytes. No excision can be seen within stromal cell populations. *Bmp7*$^{+/lacZ}$ is expressed in nephrogenic mesenchyme (E), the prospective distal end of the comma-shaped body (H), and podocytes and distal tubules of maturing nephrons (I). Proximal tubules and Bowman's capsules do not express *Bmp7*$^{+/lacZ}$. Staining in *Bmp7*$^{cre/+}$;*Rosa26*^{R} kidneys is seen throughout the nephron (F,G). *HoxB7cre* activity marks the Wolffian duct, ureteric bud and collecting ducts at E11.75 (J) and E13.5 (K). The red line in K denotes the border between the collecting duct and nephron. CB, comma-shaped body; CD, collecting duct; dist, distal tubule; Mes, metanephric mesenchyme; neph, nephron; NM, nephrogenic mesenchyme; pod, podocytes; prox, proximal tubule; PS, peripheral stroma; UB, ureteric bud; WD, Wolffian duct; B, *Bam*HI; Na, *Nae*I; Nc, *Nco*I; R, *Eco*RI.

cells of the renal vesicle. Expression can be seen only at the distal end of the developing tubule and in the podocytes. By contrast, *Bmp7*$^{cre/+}$ labeling is seen throughout the developing nephron, from the renal vesicle stage onward, demonstrating that the entire nephron is derived from *Bmp7*-expressing cells. As active *Bmp7* expression is limited to the distal tubule and podocytes, and *HoxB7cre* labeling shows that collecting duct cells are strictly confined to collecting ducts, we conclude that the renal vesicle and nascent epithelial structures are derived from *Bmp7*$^{cre/+}$-marked nephrogenic mesenchyme. This experiment conclusively demonstrates that the nephrogenic mesenchyme is the exclusive progenitor population of the nephron.

Domains of TGFβ superfamily signaling in the developing kidney

We previously described Smad protein distribution in the developing kidney (Oxburgh and Robertson, 2002). At E11.5, Smads 1, 2 and 4 are expressed only in the mesenchyme. Upon contact with the ureteric bud epithelium, expression of these Smads is downregulated in the nephrogenic mesenchyme, but remains high in uninduced mesenchyme. Subsequently, expression is limited to the peripheral and medullary stroma, mesangial cells and the proximal tubules of mature nephrons. Smad4 is expressed in the collecting duct system at low levels from approximately E11.75 onwards.

To ascertain which cells are actively transducing BMP and TGFβ signals, we performed immunohistochemistry on paraffin sections of E11.5-E13.5 kidneys using antisera detecting phosphorylated forms of Smad1 and Smad2 (Persson et al., 1998). Surprisingly, we find that the domains of activation of the two pathways are superimposable. At E11.5, signaling is seen almost exclusively in scattered cells throughout the metanephric blastema (Fig. 2A,B). By E12.5, the domains of signaling are more organized, with high levels of activation within the peripheral and mature stromal compartments. Some activation is seen in collecting ducts, but very little within nephrogenic mesenchyme (Fig. 2C,D). At E13.5, a similar pattern is observed. In addition, signaling is active in the tips and trunks of collecting ducts (Fig. 2E,F). To verify that the paucity of nuclear phospho-Smad staining in the nephrogenic mesenchyme was not due to our staining method, we performed immunohistochemistry using an antigen unmasking protocol (Schnabel et al., 2001). No difference could be seen in phospho-Smad staining using this protocol, despite homogenous nephrogenic mesenchyme staining using Pax2 antiserum as a control on adjacent sections (data not shown).

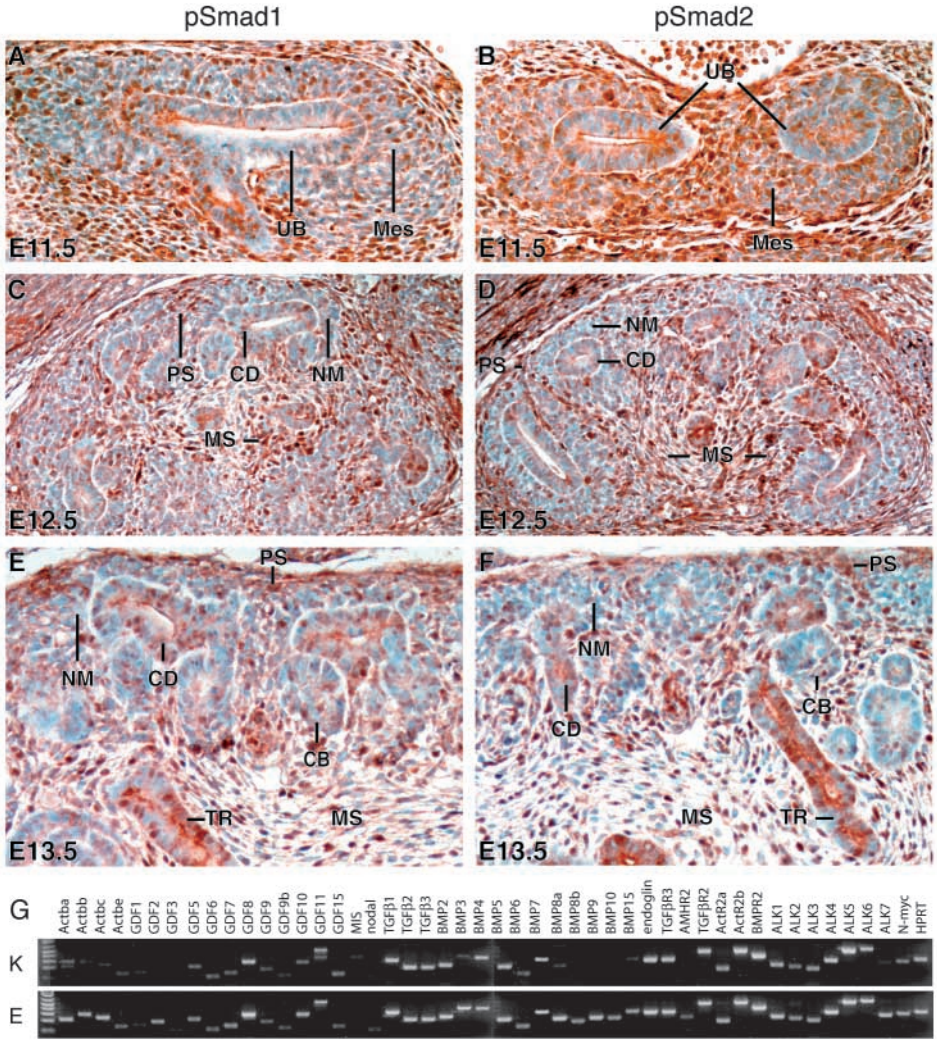

Fig. 2. Localization of active BMP and TGFβ signal transduction in the developing kidney. Nuclear immunohistochemical staining for phospho-Smad1 (pSmad1) and phospho-Smad2 (pSmad2) identifies cells actively responding to BMP and TGFβ signals, respectively. At E11.5 (A,B), activation is mainly within the metanephric mesenchyme, with responding cells disseminated throughout the mesenchyme. The ureteric bud contains a small number of positive cells. At E12.5 (C,D), pathway activation is predominantly within the peripheral and mature stroma. Few positive cells are seen in nephrogenic mesenchyme and collecting ducts. At E13.5 (E,F), activation is seen in peripheral and mature stroma. Nephrogenic mesenchyme and epithelial structures such as comma-shaped bodies show little staining. Tips and trunks of collecting ducts show activation. (G) RT-PCR for expression of components of the TGFβ superfamily pathway in (K) E11.5 kidneys and (E) control E17.5 embryos. CD, collecting duct; CB, comma-shaped body; Mes, metanephric mesenchyme; MS, mature stroma; NM, nephrogenic mesenchyme; TR, collecting duct trunk; UB, ureteric bud.

To comprehensively assess the expression of TGFβ superfamily ligands and their cognate receptors during kidney development, we performed RT-PCR on RNA from E11.5 kidneys (Fig. 2G). This stage was chosen for analysis because it is morphologically the simplest. *Gdf5*, *6*, *7*, *8*, *10*, *11* and *15*, *Tgfb1*, *2* and *3*, and *Bmp2*, *4*, *5*, *6* and *7* are expressed, as is the full complement of receptors, with *Alk7* showing very low level expression. Taken together with previous protein expression studies (Bosukonda et al., 2000; Oxburgh and Robertson, 2002; Pelton et al., 1991; Vukicevic et al., 1994), it is apparent that both TGFβ and BMP signaling is extensive at E11.5. However, pSmad immunohistochemistry reveals mosaic signaling in cells of the metanephric mesenchyme, and limited activation in the trunk and tips of the collecting duct system, indicating that regulation of the pathway may be determined by factors other than ligand, receptor and Smad availability.

Inactivation of *Smad4* in the collecting ducts

HoxB7cre was introduced into the *Smad4* conditional background to generate *HoxB7cre;Smad4*$^{-/CA}$ mice that were born at approximately Mendelian frequencies (21%, *n*=42). Mutant mice were phenotypically normal at 6 weeks of age, but by 8 weeks, 3 out of 8 mutant mice had died. Kidneys from these mice did not display overt morphological defects (data not shown), and *HoxB7cre;Smad4*$^{-/CA}$ mice are to be assessed for kidney function. These results will be reported elsewhere. At E16.5, no difference between mutant and wild-type kidneys was documented, either macroscopically or histologically (Fig. 3B). Loss of Smad4 in the collecting ducts thus has no effect on kidney development up to E16.5.

Inactivation of *Smad4* in the mesenchyme

We next employed the *Bmp7*$^{cre/+}$ strain to eliminate *Smad4* in the mesenchyme. *Bmp7*$^{cre/+}$ was introduced into the *Smad4* conditional background to generate *Bmp7*$^{cre/+}$*;Smad4*$^{-/CA}$ mice. No *Bmp7*$^{cre/+}$*;Smad4*$^{-/CA}$ pups were identified one week after birth (*n*=20). At P1, a low frequency of *Bmp7*$^{cre/+}$*;Smad4*$^{-/CA}$ were identified (7%, the expected Mendelian ratio is 25%, *n*=42). At E17.5, Mendelian ratios of *Bmp7*$^{cre/+}$*;Smad4*$^{-/CA}$ embryos were observed (*n*=52). Examination of mutant kidneys revealed severely disturbed development. The kidneys were approximately half the volume of wild type, and displayed sporadic cyst formation and hydroureter (Fig. 3C). Despite an unusual clustering of glomeruli and occasional cystic Bowman's spaces, the capillary tufts, podocyte layers and mesangial components appear normal. In addition, extensive tubules are associated with glomeruli. The relatively normal development of these mature structures indicates that Smad4 is not required for their morphogenesis.

Close examination of collecting ducts at E16.5 revealed that the tips are surrounded by variable amounts of nephrogenic mesenchyme, with approximately half of the tips entirely devoid of these cells. This feature of the phenotype is also apparent at E14.5, where a prominent thickening of the cell layer between the nephrogenic mesenchyme and the kidney capsule is seen (Fig. 3E). In wild-type kidneys, this single layer

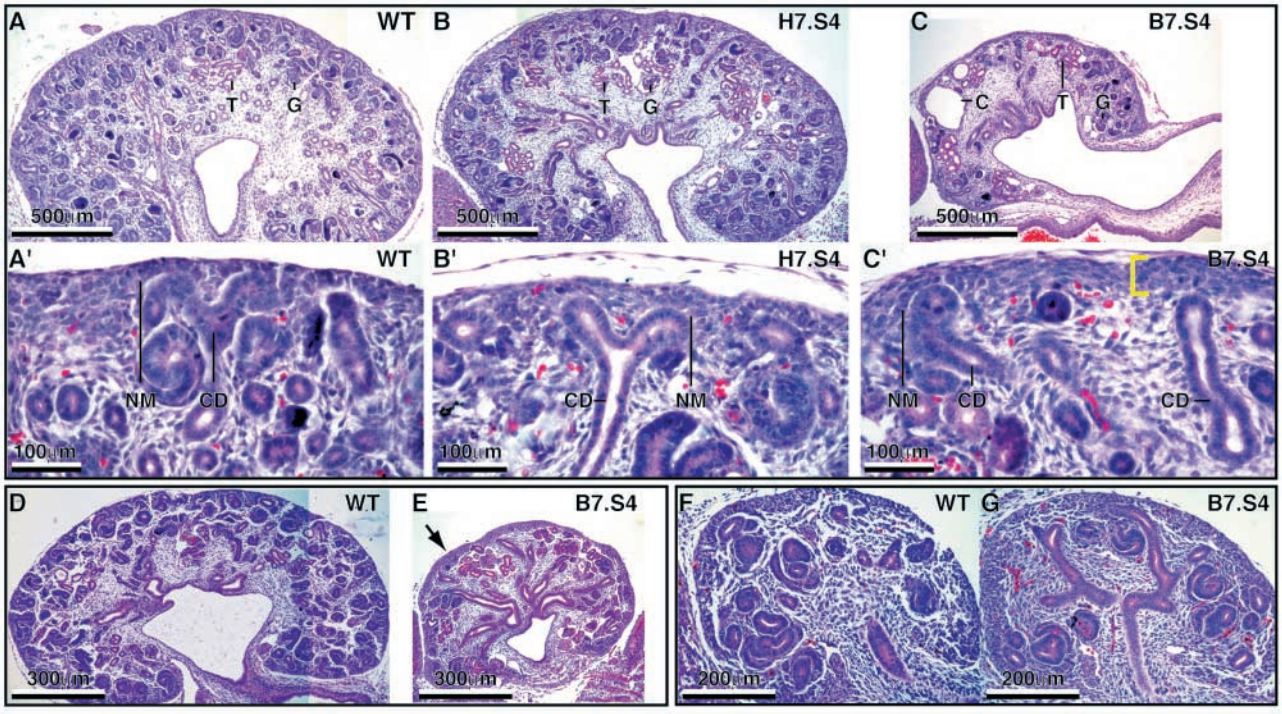

Fig. 3. Morphology of *Bmp7*$^{cre/+}$*;Smad4*$^{-/CA}$ and *HoxB7cre;Smad4*$^{-/CA}$ kidneys. (A-C) Sagittal sections of E16.5 kidneys. (A′-C′) High magnification images of the cortical zone of each section. Kidneys of *HoxB7cre;Smad4*$^{-/CA}$ (H7.S4) kidneys (B) are indistinguishable from wild type (A). *Bmp7*$^{cre/+}$*;Smad4*$^{-/CA}$ (B7.S4) kidneys (C) display hydroureter and cyst formation. Nephrogenic mesenchyme is missing from the majority of collecting duct tips, and the cortical cell layer is thickened (bracket in C′). E14.5 *Bmp7*$^{cre/+}$*;Smad4*$^{-/CA}$ kidneys (E) are smaller than wild-type controls (D) and display a prominent thickening of the cortical layer normally composed of nephrogenic mesenchyme and peripheral stroma (arrow). E12.5 *Bmp7*$^{cre/+}$*;Smad4*$^{-/CA}$ kidneys (G) are of comparable size to wild-type controls (F). CD, collecting duct; C, cyst; G, glomerulus; NM, nephrogenic mesenchyme; T, tubules.

of peripheral stromal cells is located between the nephrogenic mesenchyme and the kidney capsule, and populates the clefts between aggregates of nephrogenic mesenchyme. At E12.5, the lack of nephrogenic mesenchyme in mutants is less obvious, but a marked thickening of the cortical cell layer is evident compared with wild type. Extensive cell death can be seen in cortical regions between aggregates of nephrogenic mesenchyme (Fig. 7A-F). A reduction in the number of collecting ducts can be seen in the mutant, with the average number of peripheral collecting duct tips counted in sagittal sections from the center of three individual kidneys being: 7(±1) in wild type and 6(±1) in mutants at E12.5; 20(±2) in wild type and 8(±1) in mutants at E14.5; and 28(±2) in wild type and 9(±2) in mutants at E16.5.

Nephrogenic mesenchyme is disorganized and prematurely depleted in *Bmp7$^{cre/+}$;Smad4$^{-/CA}$* kidneys

We next examined *Bmp7$^{cre/+}$;Smad4$^{-/CA}$* kidneys at E14.5 and E16.5 by in situ hybridization with a panel of diagnostic markers. At E14.5, *Ret* expression is restricted to the tips of collecting ducts (Fig. 4A). Mutant kidneys show *Ret* expression, indicating that branching occurs normally. *Pax2* is expressed throughout the collecting ducts in wild-type kidneys, and this pattern is maintained in the mutant (Fig. 4C,D). *Pax2* and *Wt1* expression were used to assess the degree of mesenchyme development in mutant kidneys. In the wild-type kidney, *Wt1* and *Pax2* are expressed in the nephrogenic mesenchyme surrounding the collecting duct tips (Fig. 4C,E). In addition, *Wt1* marks the podocyte layer of the glomerulus. Mutant kidneys display an overall paucity of nephrogenic mesenchyme, as demonstrated by weak and patchy expression of *Pax2*. *Wt1* expression is not localized to the nephrogenic mesenchyme in the mutant, but is distributed throughout the cortical layer (Fig. 4E,F). By contrast, glomerular *Wt1* expression appears normal. Taken together, these findings indicate that, in the absence of *Smad4*, some normal condensation of mesenchyme does occur, leading to the development of a limited number of mature epithelial structures.

The homogenous distribution of *Wt1* within the expanded

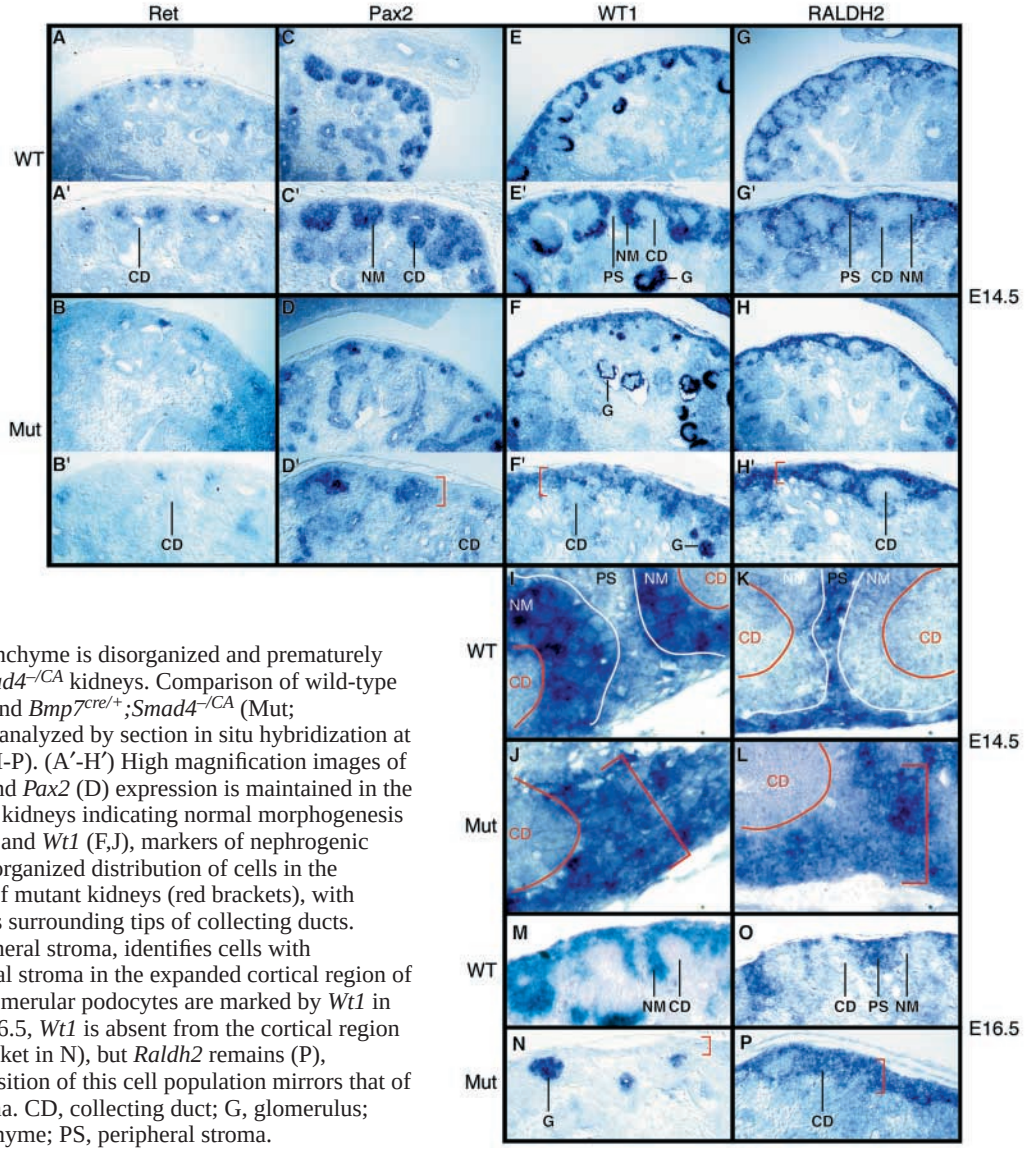

Fig. 4. Nephrogenic mesenchyme is disorganized and prematurely depleted in *Bmp7$^{cre/+}$;Smad4$^{-/CA}$* kidneys. Comparison of wild-type (WT; A,C,E,G,I,K,M,O) and *Bmp7$^{cre/+}$;Smad4$^{-/CA}$* (Mut; B,D,F,H,J,L,N,P) kidneys analyzed by section in situ hybridization at E14.5 (A-L) and E16.5 (M-P). (A′-H′) High magnification images of cortical regions. *Ret* (B) and *Pax2* (D) expression is maintained in the collecting ducts of mutant kidneys indicating normal morphogenesis of this structure. *Pax2* (D) and *Wt1* (F,J), markers of nephrogenic mesenchyme, reveal a disorganized distribution of cells in the expanded cortical region of mutant kidneys (red brackets), with occasional clusters of cells surrounding tips of collecting ducts. *Raldh2*, a marker of peripheral stroma, identifies cells with characteristics of peripheral stroma in the expanded cortical region of mutant kidneys (H,L). Glomerular podocytes are marked by *Wt1* in mutant kidneys (F). At E16.5, *Wt1* is absent from the cortical region of the mutant kidney (bracket in N), but *Raldh2* remains (P), suggesting that the composition of this cell population mirrors that of wild-type peripheral stroma. CD, collecting duct; G, glomerulus; NM, nephrogenic mesenchyme; PS, peripheral stroma.

cortical layer of mutant kidneys at E14.5 is noteworthy because *Wt1* expression is normally strictly localized to the nephrogenic mesenchyme (Fig. 4F,I). This could be explained either by the presence of a cell type expressing both stromogenic and nephrogenic markers, or by ectopic placement of nephrogenic mesenchyme within the peripheral stroma. Comparison of expression of the peripheral stromal marker *Raldh2* with *Wt1* at E14.5 shows co-localization in the expanded cortical layer (Fig. 4I-L). However, at E16.5 the cortical cell layer remains expanded but expresses *Raldh2* almost exclusively (Fig. 4N,P). A population of cells with characteristics of both nephrogenic mesenchyme and stroma are thus replaced by cells of a stromal phenotype, possibly indicating that an immature *Wt1*- and *Raldh2*-expressing population of cells is being exhausted through nephrogenesis.

Nephrogenic mesenchyme and stroma are incompletely segregated in *Bmp7$^{cre/+}$;Smad4$^{-/CA}$* kidneys

In order to understand whether the distribution of stroma and nephrogenic mesenchyme is disturbed from the outset of metanephric development, we analyzed gene expression in E11.5 and E12.5 mutant kidneys. At E11.5, the metanephric mesenchyme of mutant kidneys expresses both *Wt1* and *Pax2*, indicating normal patterning (Fig. 5A-D). Expression of *Raldh2* is seen throughout the mesenchyme, and is excluded from condensates surrounding ureteric bud tips, an expression pattern indistinguishable from that of wild type (Fig. 5E,F). Strong expression of *Lhx1* in foci within the mesenchyme indicates the formation of epithelial structures at comparable times in wild-type and mutant kidneys (Fig. 5G,H). We

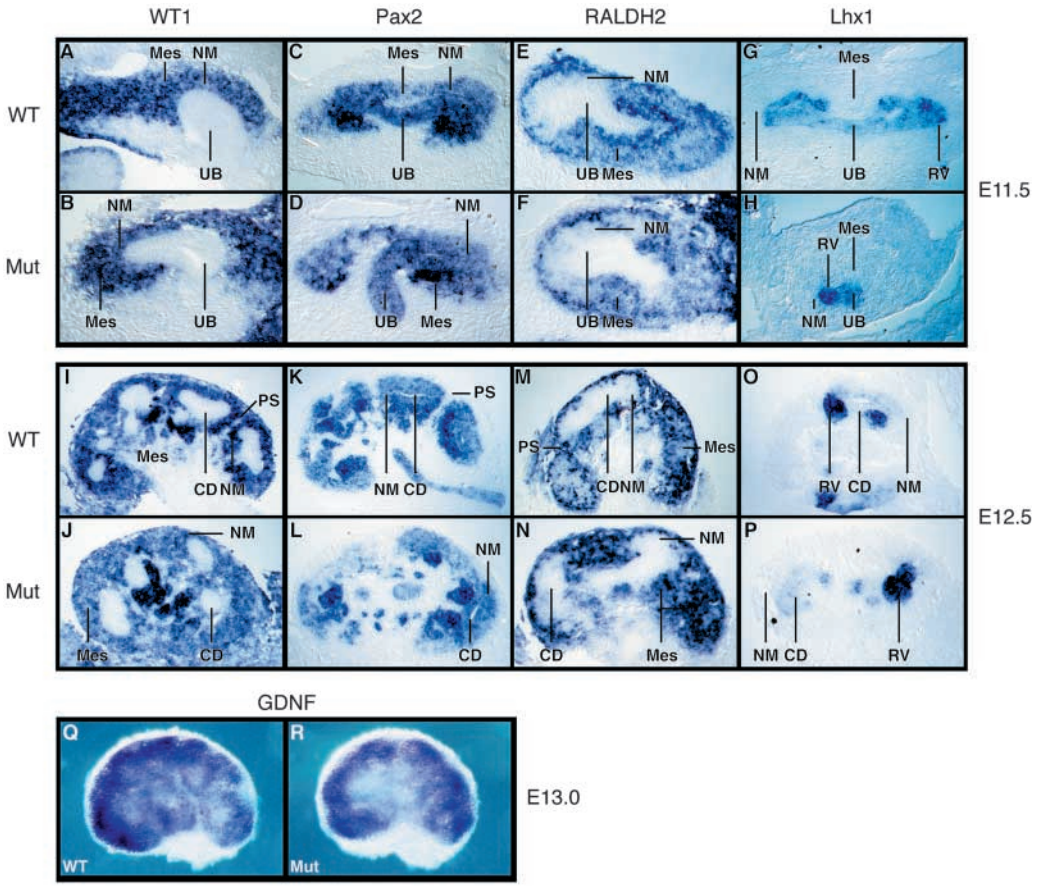

Fig. 5. Nephrogenic mesenchyme and stroma are incompletely segregated in *Bmp7$^{cre/+}$;Smad4$^{-/CA}$* kidneys. Comparison of wild-type (WT; A,C,E,G,I,K,M,O,Q) and *Bmp7$^{cre/+}$;Smad$^{-/CA}$* (Mut; B,D,F,H,J,L,N,P,R) at E11.5 (A-H), E12.5 (I-P) and E13.0 (Q,R). At E11.5, expression of *Wt1* (B) and *Pax2* (D) in mutant kidneys is indistinguishable from that of wild type (A,C), indicating that the metanephric blastema is appropriately patterned. *Raldh2* (F) reveals a distribution of stromal cells in mutants that is comparable to wild type (E). Expression of *Lhx1* (H) at E11.5 indicates that maturing structures such as renal vesicles appear at approximately the same time in mutant kidneys as they do in wild type (G). At E12.5, expression of *Wt1* (J) reveals disorganization of the nephrogenic mesenchyme that normally forms around collecting duct tips. Expression of *Wt1* is widespread in the wild-type mesenchyme at E12.5 (I), and *Wt1*-negative peripheral stroma can only be seen in occasional sections. *Pax2* expression clearly demarcates nephrogenic mesenchyme and nascent epithelia from stromal cells in the wild type (K). Mutant kidneys show a paucity of nephrogenic mesenchyme and no clear demarcation of stromal cells (L). *Raldh2* expression is confined to the stromal cell compartment of the wild-type kidney (M), and is excluded from nephrogenic mesenchyme and collecting ducts. In the mutant (N), *Raldh2* expression is spread throughout the majority of the mesenchyme, and is excluded from the limited nephrogenic mesenchyme population and collecting ducts. *Lhx1* expression reveals several renal vesicles per section in the wild type (O), but only a limited number in the mutant (P). At E13.0, Gdnf expression is comparable in the wild type (Q) and the mutant (R). CD, collecting duct; G, glomerulus; Mes, metanephric mesenchyme; NM, nephrogenic mesenchyme; PS, peripheral stroma; RV, renal vesicle; UB, ureteric bud.

therefore conclude that the distribution of cell types in E11.5 mutant kidneys is normal.

At E12.5, the ureteric bud has branched, and induces the condensation of nephrogenic mesenchyme around collecting duct tips. These condensates are clearly marked by *Wt1* expression in the wild type (Fig. 5I). In mutant kidneys, *Wt1* expression is distributed diffusely throughout the mesenchyme, and few foci of nephrogenic mesenchyme are seen (Fig. 5J). At this stage only a few *Wt1*-negative presumptive stromal cells are observed at the periphery of the kidney. *Pax2* expression identifies a more limited subset of mesenchyme cells at E12.5, and in the wild type, a *Pax2*-negative layer of cells surrounding nephrogenic mesenchyme aggregates is apparent (Fig. 5K). By contrast, mutant kidneys display a disorganization of *Pax2*-positive cells, with large expanses of the mesenchyme devoid of *Pax2* expression (Fig. 5L). *Raldh2* is expressed in a domain that is complementary to *Pax2* in the wild-type kidney, marking cells surrounding aggregates of nephrogenic mesenchyme (Fig. 5M). This stromal cell population is expanded in the mutant, and overlaps with *Wt1* expression (Fig. 5N). The number of epithelial structures marked by *Lhx1* is reduced in the mutant kidney (Fig. 5P). In summary, a paucity of bona fide *Wt1*- and *Pax2*-expressing nephrogenic mesenchyme at E12.5 is accompanied by a marked overrepresentation of *Wt1*- and *Raldh2*-expressing mesenchyme. As we find that there is significant overlap between the domains of *Wt1* and *Raldh2* expression at early time-points in the normal kidney, we suggest that *Wt1*- and *Raldh2*-expressing cells in the early wild-type mesenchyme are normally recruited into *Wt1*- and *Pax2*-expressing, but *Raldh2*-negative, nephrogenic mesenchyme aggregates upon induction. Loss of Smad4 in the mesenchyme impairs this inductive process and the immature population of mesenchyme persists until it is depleted at around E16.5.

In order to ascertain whether the reduced number of collecting duct branches seen in mutant kidneys could be caused by a lack of expression of *Gdnf*, in situ hybridization for this gene was carried out at E13.0, a time point at which the depletion of nephrogenic mesenchyme is not yet pronounced. Mutant kidneys showed *Gdnf* expression similar to wild type (Fig. 5Q,R), indicating that this is not the case.

Lineage analysis of *Bmp7^{cre};Smad4$^{-/CA}$* kidneys

To determine the ontogeny of cells within the expanded cortical layer of mutant kidneys, we next introduced the *ROSA26^{R}* conditional reporter into either the *Bmp7$^{cre/+}$;Smad4$^{-/CA}$* or the *Bmp7$^{cre/+}$* backgrounds (hereafter referred to as mutant and wild-type, respectively). Kidneys were analyzed at E11.5, E12.0, E14.5 and E16.5 for *lacZ* activity. In the mutant, cells derived from *Smad4*-deficient progenitors are labeled by *lacZ* activity. In both wild-type and mutant kidneys, as expected, the collecting ducts are homogenously stained at all time-points analyzed. However, comparison of the mesenchymal and stromal components of wild-type and mutant kidneys reveals significant differences. At E11.5, mutant mesenchyme is indistinguishable from wild type, labeled cells being distributed through the blastema but primarily localized to the area immediately surrounding ureteric bud tips (Fig. 6B). By E12.0 in wild-type kidneys, labeled cells are closely associated with collecting duct tips and display the morphological characteristics of nephrogenic mesenchyme (Fig. 6C,E). By contrast, there is significant mixing of labelled, and thus *Smad4*-deficient, cells with unlabeled cells of other lineages around the collecting duct tips of the mutant (Fig. 6D,F). Also, labeled cells are distributed through the mesenchyme and do not appear to condense tightly in the vicinity of duct tips. In E14.5 wild-type kidneys, labeled cells surround the tips of collecting ducts, comprising the nephrogenic mesenchyme lineage (Fig. 6G). No labeled cells are seen within the peripheral stromal layer separating the nephrogenic

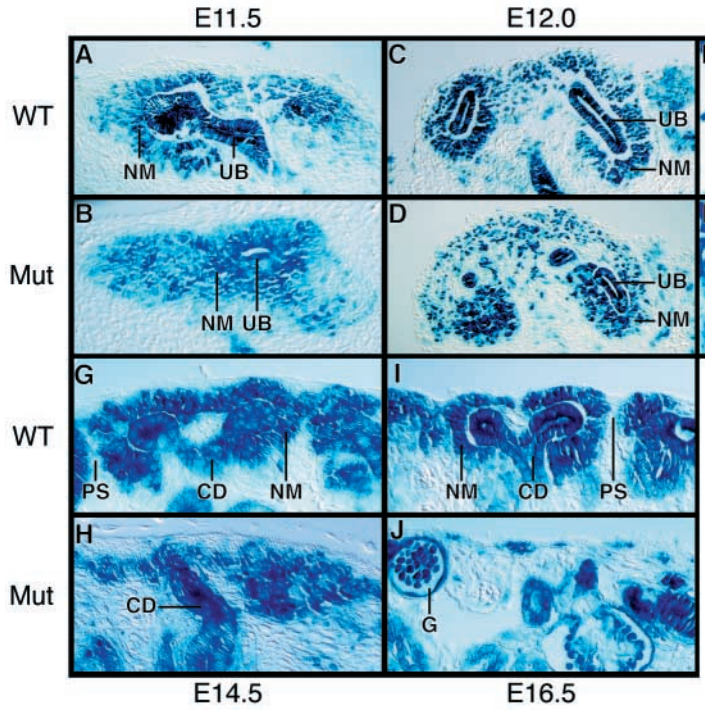

Fig. 6. Lineage analysis of *Bmp7$^{cre/+}$;Smad$^{-/CA}$* kidneys. The *ROSA26^{R}* reporter was introduced into the *Bmp7$^{cre/+}$*(WT) and *Bmp7$^{cre/+}$;Smad4$^{-/CA}$* (Mut) backgrounds. At E11.5, the ureteric bud and condensing mesenchyme of wild-type (A) and mutant (B) kidneys are labeled by *lacZ* expression. At E12.0 (C,E), all cells within the nephrogenic mesenchyme of wild-type kidneys are labeled, whereas there is significant mixing of labeled and unlabeled cells in the mutant (D,F). Labeled and unlabeled cells are distributed throughout the mesenchyme of mutant kidneys. At E14.5, nephrogenic mesenchyme is labeled in wild-type kidneys (G), and the stroma surrounding mesenchymal condensates is unlabeled. In mutant kidneys (H), the limited nephrogenic mesenchyme that can be seen is labeled, and there is a disorganized distribution of labeled cells throughout the cortical layer, which is composed of a mixture of labeled and unlabeled cells. At E16.5, nephrogenic mesenchyme is labeled, and unlabeled stromal cells are more obvious in wild-type kidneys (I). In mutant kidneys, a few remaining labeled cells lie within the otherwise unlabeled cortical layer (J). Ectopically placed glomeruli are prominent. CD, collecting duct; G, glomerulus; NM, nephrogenic mesenchyme; PS, peripheral stroma; UB, ureteric bud.

mesenchyme and the kidney capsule. However, the mutant displays a reduced overall volume of nephrogenic mesenchyme, and labeled *Smad4*-deficient cells are ectopically located within the expanded cortical layer (Fig. 6H). However, this localization is transient because marked cells are largely missing from the cortical layer of mutants at E16.5 (Fig. 6J).

In summary, conditional deletion of *Smad4* in metanephric mesenchyme leads to a quantitative reduction in nephrogenesis and the arrest of kidney development by approximately E16.5. Relatively normal epithelial structures are found within mutant kidneys, indicating that the developmental program leading to nephron formation is unperturbed. By marker and lineage analysis, metanephric development is initiated normally in mutants, but organization of the mesenchyme is perturbed, concomitant with the initiation of branching of the collecting ducts. Nephrogenic mesenchyme does not associate closely with collecting duct tips, and an immature population of *Wt1*- and *Raldh2*-expressing mesenchyme remains at the periphery of the kidney. This population is depleted as nephrogenesis proceeds, and the kidney is largely devoid of these cells by E16.5.

Bmp7$^{cre/+}$;*Smad4*$^{-/CA}$ kidneys display increased peripheral cell death

To understand the role of cell death in the mutant phenotype, we performed a careful histological analysis for pyknotic nuclei on serial sections of wild-type and mutant kidneys. At E12.0, E14.5 and E16.5, clusters of dead cells can be seen in the thickened areas of the mesenchyme at the periphery of mutant kidneys (Fig. 7B,D,F). These clusters of dead cells localize to regions distant from collecting duct tips. This contrasts with the patterns of cell death observed in wild-type kidneys (Fig. 7A,C,E), in which only sporadic pyknotic nuclei can be seen at the periphery. In areas of mutant kidneys in which recognizable nephrogenic mesenchyme is organized around collecting duct tips, pyknotic nuclei could be seen at a frequency comparable with that of wild type, indicating that the depletion of nephrogenic mesenchyme does not occur specifically through cell death.

To assess the degree of proliferation, we immunostained sections for the presence of proliferating cell nuclear antigen (PCNA). Proliferation in the cortical region of the wild-type kidney is distributed evenly throughout the collecting ducts, nephrogenic mesenchyme and peripheral stroma (Fig. 7G,I). This pattern of proliferation is maintained in the mutant. Importantly, collecting ducts display an even distribution of proliferating cells, indicating that the primary cause for the paucity of collecting ducts is not an innate failure of the collecting duct epithelium to proliferate.

Bmp7$^{cre/+}$;*Smad4*$^{-/CA}$ metanephric mesenchyme responds to induction in vitro

To explore whether the disturbed aggregation of nephrogenic mesenchyme is due to a defect in the induction of mutant

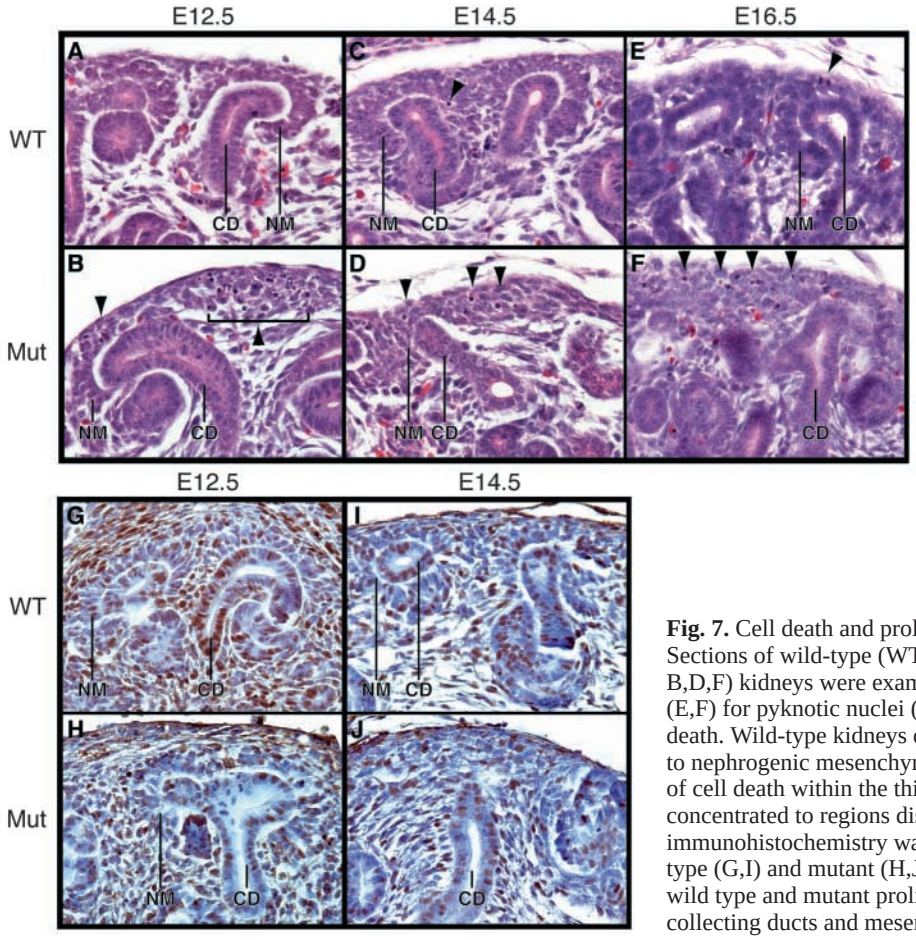

Fig. 7. Cell death and proliferation in *Bmp7*$^{cre/+}$;*Smad4*$^{-/CA}$ kidneys. Sections of wild-type (WT; A,C,E) and *Bmp7*$^{cre/+}$;*Smad4*$^{-/CA}$ (Mut; B,D,F) kidneys were examined at E12.5 (A,B), E14.5 (C,D) and E16.5 (E,F) for pyknotic nuclei (marked by arrowheads) as markers of cell death. Wild-type kidneys display only sporadic single dead cells adjacent to nephrogenic mesenchyme. By contrast, mutant kidneys show clusters of cell death within the thickened peripheral cell layer, mainly concentrated to regions distant from collecting duct tips. PCNA immunohistochemistry was used to identify proliferating cells in wild-type (G,I) and mutant (H,J) kidneys at E12.5 (G,H) and E14.5 (I,J). Both wild type and mutant proliferating cells are similarly distributed in collecting ducts and mesenchyme.

mesenchyme, we used an in vitro culture system to compare the inducibility of wild-type and mutant mesenchyme at E11.5, using LiCl as an inducing agent (Davies and Garrod, 1995) (Fig. 8). After enzymatic separation, mesenchyme was cultured on filter rafts in the presence or absence of LiCl for 72 hours. Mutant mesenchyme was induced, but attained consistently smaller volumes than wild type at the end of the culture period (n=10). Histological analysis of induced mesenchyme revealed that epithelial structures formed both in wild-type and mutant mesenchyme, with wild-type mesenchyme developing slightly more complex tubular epithelial structures (Fig. 8E,F). Immunostaining of mesenchyme revealed an appropriate deposition of laminin (Fig. 8G,H). This result was reproduced upon co-culture of mesenchyme with the heterologous inducer spinal cord (data not shown). We conclude from this assay that *Bmp7*$^{cre/+}$*;Smad4*$^{-/CA}$ mesenchyme is fully competent to respond to inducing signals.

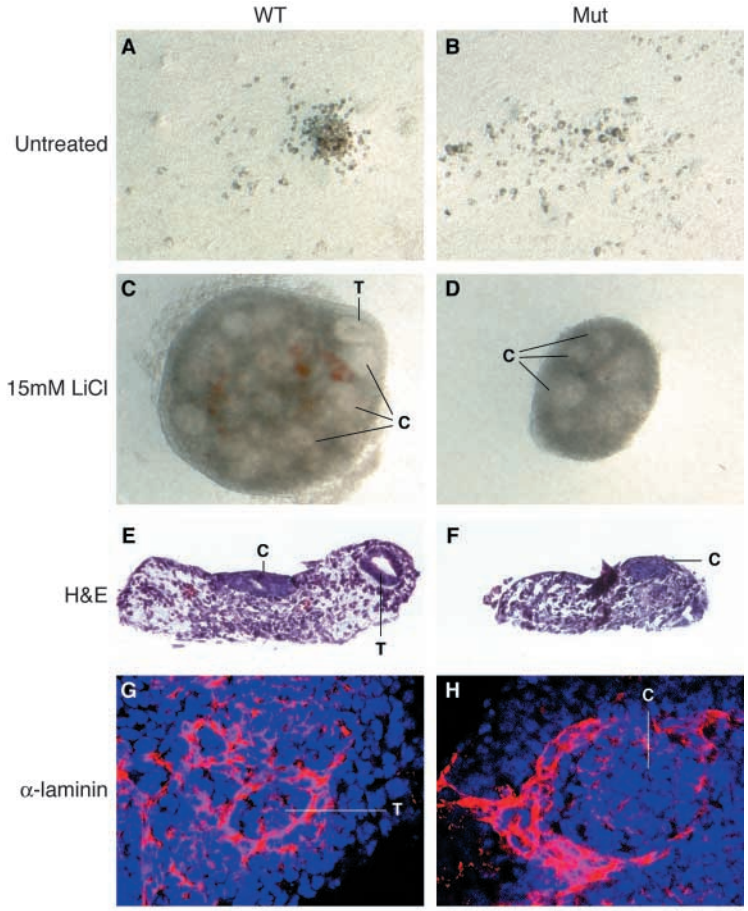

Fig. 8. *Bmp7*$^{cre/+}$*;Smad4*$^{-/CA}$ metanephric mesenchyme responds to induction in vitro. Wild-type (WT) and *Bmp7*$^{cre/+}$*;Smad4*$^{-/CA}$ (Mut) mesenchyme was cultured with and without LiCl, a potent nephrogenic inducer. Untreated mesenchyme rapidly underwent cell death (A,B), whereas treated mesenchyme survived and underwent nephrogenic induction (C,D). Photographs were taken at the same magnification, and the size difference between induced wild-type and mutant mesenchyme is representative. Histological analysis revealed the presence of epithelial condensates within both wild-type (E) and mutant (F) mesenchyme, and the development of tubular structures within the wild type. Basal deposition of laminin surrounding condensates was confirmed by fluorescent immunostaining (G,H). C, condensate; T, tubule.

Discussion

In comparison to the large number of TGFβ superfamily ligands that have been shown to affect kidney development, a surprisingly limited number of mutations in TGFβ pathway members have been shown to affect development of this organ in vivo. Gene expression analysis of ligands and receptors in this study and others (Dudley and Robertson, 1997; Oxburgh and Robertson, 2002; Pelton et al., 1991; Plisov et al., 2001) demonstrates that many pathway members are expressed simultaneously, raising the possibility that extensive redundancy obscures the role of this pathway in kidney development. Smad4 is an integral component of the signal transduction cascade downstream of ligand-receptor interactions, mediating the nuclear translocation of phosphorylated receptor-associated Smads and allowing them to participate in transcriptional regulation (Lagna et al., 1996; Xiao et al., 2003). Thus, *Smad4* represents a genetically tractable 'bottleneck' in the TGFβ signaling pathway and we have used conditional inactivation of this gene in two different cell populations to further characterize the roles of TGFβ superfamily signaling in early kidney development.

Lineage relationships in the developing kidney

As the Cre-loxP system induces heritable labeling of cells in the *ROSA26*^{R} conditional reporter strain, it provides a convenient tool for lineage analysis. The predicted domains of expression for the Cre-expressing lines used in this study are: (1) the ureteric bud and collecting duct system for *HoxB7cre* (Srinivas et al., 1999); and (2) the ureteric bud, collecting duct system and nephrogenic mesenchyme for *Bmp7*$^{cre/+}$ (Godin et al., 1998). Because the expression domains of *HoxB7* and *Bmp7* overlap exactly in the ureteric bud and collecting ducts, it is possible to deduce the fate of the nephrogenic mesenchyme by comparison of the two.

Two main points regarding lineage relationships between cell populations within the metanephros emerge from this study. The first is that cells of ureteric bud origin do not contribute in significant numbers to the mesenchyme, as has previously been suggested (Herzlinger et al., 1993). The few *lacZ*-expressing cells that can be seen outside the collecting ducts in *HoxB7cre;R26*^{R} kidneys are confined to the medullary stroma, and are never seen within the nephrogenic mesenchyme or mesenchymal structures such as renal vesicles or nephric tubules. A possible reason for the discrepancy between our findings and those of Herzlinger et al. (Herzlinger et al., 1993) is the fact that the latter study was performed in organ culture using cell labeling, which is a less accurate technique than in vivo fate mapping. Also, it cannot be excluded that cell lineages are less strictly segregated in cultured organs, perhaps owing to the removal of surrounding tissue. The second finding is that cells of the nephrogenic mesenchyme labeled by *Bmp7*$^{cre/+}$ are restricted to the nephrogenic lineage; only a scattering of labeled cells can be found within the medullary stroma. The same scattering of labeled cells was seen with *HoxB7cre*,

suggesting that these represent cells that have migrated into the kidney. Commitment to either stromal or nephrogenic lineages thus occurs prior to induction and the condensation around collecting duct tips, if indeed cells of these lineages are derived from the same progenitor. As labeled cells are seen in mosaic fashion in the early metanephric mesenchyme and subsequently consolidate around collecting duct tips, we conclude that segregation of nephrogenic and stromal progenitors occurs at this early time point. Future studies using Cre transgenes that label the stromal cell population will test whether cells of stromal origin incorporate into the nephrogenic mesenchyme and will clarify whether these lineages derive from a common precursor.

The role of *Smad4* in collecting duct epithelium

In the ureteric bud, onset of BMP and TGFβ pathway activation is relatively late, with appreciable levels of phosphorylated Smads being detectable first at E12.5 in collecting duct trunks. Removal of *Smad4* within this tissue has no effect on kidney development up to E16.5. This is a surprising result, as several studies have shown that BMP and TGFβ ligands applied to E11.5 kidney explants inhibit growth and branching of the collecting duct system, and it has therefore been assumed that these pathways are involved in collecting duct morphogenesis (Bush et al., 2004; Clark et al., 2001; Piscione et al., 1997; Ritvos et al., 1995; Rogers et al., 1993). Interestingly, a study in which constitutively activated Alk3 was expressed in collecting ducts using the *HoxB7* enhancer-promoter revealed an inhibitory effect of BMP pathway activation on collecting ducts, confirming these in vitro findings (Hu et al., 2003). However, it was found that phosphorylated Smad1 complexes with β-catenin leading to activation of the Wnt pathway, presumably without the participation of Smad4. It thus seems likely that TGFβ superfamily signals are transduced through Smad4-independent pathways in the collecting duct. Further studies using inhibitors of alternative pathways that have been shown in other organ systems to be activated by TGFβ superfamily ligands, such as the MAP kinase cascade, may shed additional light on this mechanism of signal transduction.

The role of *Smad4* in metanephric mesenchyme

The earliest co-localization of $Bmp7^{cre/+}$ and *Smad4* expression in kidney development is limited to a dispersed population of cells within the metanephric blastema at E11.0-E11.5. Upon induction of the blastema by the ureteric bud, the population of $Bmp7^{cre/+}$ labeled cells coalesces around the ureteric bud to form the nephrogenic mesenchyme, and from this point onward $Bmp7^{cre/+}$ labeled cells are confined to the nephrogenic mesenchyme and its derivatives. Nephrogenic mesenchyme expresses very little *Smad4*, and shows limited pathway activation (Oxburgh and Robertson, 2002). We therefore conclude that the phenotype seen upon loss of *Smad4* in dispersed cells of the metanephric blastema occurs prior to formation of the nephrogenic mesenchyme. However, it cannot be excluded that the very small number of nephrogenic mesenchyme cells displaying *Smad4* expression at later points in development contribute to the phenotype.

The profound effects of $Bmp7^{cre/+}$ inactivation of *Smad4* can be divided into two categories: those that phenocopy previously described TGFβ superfamily pathway mutants, and novel effects. Like the *Bmp7* homozygous null mutant, the $Bmp7^{cre/+};Smad4^{-/CA}$ mutant displays ectopic cell death at the periphery of the kidney at E12.5, and premature depletion of nephrogenic mesenchyme. The *Bmp7* mutant phenotype originates from a lack of *Bmp7* signaling to the progenitor cell population of the developing kidney (Dudley et al., 1999). That this phenotype can be recapitulated by the inactivation of *Smad4* in *Bmp7*-expressing cells implies that these progenitors reside within the nephrogenic mesenchyme. Bmp7 thus appears to act in an autocrine manner to promote progenitor survival. The early and mosaic appearance of the *Bmp7*-expressing cell population suggests that the metanephric blastema is composed of distinct cell types, and that the first inductive contact with the ureteric bud serves as a signal to organize nephrogenic progenitors around the inducer.

The expansion of the cortical layer of $Bmp7^{cre/+};Smad4^{-/CA}$ mutant kidneys is previously undescribed in any TGFβ superfamily mutation. Our analysis of *Wt1* and *Pax2* expression in wild-type kidneys reveals that these markers are expressed in partially overlapping cell populations in the mesenchyme. At E11.5, *Wt1* is expressed throughout the metanephric blastema, whereas *Pax2* expression is localized mainly to mesenchyme surrounding ureteric bud tips. At E12.5, *Wt1* expression is still seen in the majority of the mesenchyme, and expression is intensified in nephrogenic mesenchyme surrounding collecting duct tips. *Pax2* expression is limited to nephrogenic mesenchyme and maturing epithelial structures. The *Wt1*-expressing but *Pax2*-negative cell population at the periphery of the kidney overlaps with cells expressing *Raldh2*, a stromal cell marker. This cell population, with characteristics of both nephrogenic mesenchyme and stroma, is greatly expanded in $Bmp7^{cre/+};Smad4^{-/CA}$ mutant kidneys from E12.5 to E14.5. We suggest that this immature precursor of both nephrogenic mesenchyme and peripheral stroma remains uninduced in the mutant kidney, and is gradually recruited into the nephrogenic and stromal lineages. Induction by collecting duct tips recruits mesenchyme into the nephrogenic lineage, thus leaving the cortical region of the mutant kidney devoid of *Wt1*-expressing cells by E16.5. Alternatively, co-expression of *Wt1* and *Raldh2* in cells of the thickened cortical layer could indicate the presence of an immature population of cells committed to the nephrogenic lineage but expressing certain stromal cell markers that are downregulated upon induction into the nephrogenic mesenchyme. Interestingly, focal cell death can be seen in areas of the expanded peripheral cell layer distant from collecting duct tips, indicating that this cell population is dependent on signals from collecting ducts for its survival. The cortical expansion of a population of cells with both nephrogenic and stromal characteristics is also seen in compound mutants of the retinoic acid receptors α and β2 (Mendelsohn et al., 1999). This phenotype can be rescued by transgenic overexpression of *Ret* in collecting ducts, conclusively showing that the mesenchyme phenotype is secondary to a collecting duct defect. The similarity of this primarily collecting duct phenotype to the mesenchymal $Bmp7^{cre/+};Smad4^{-/CA}$ phenotype supports our hypothesis, as one would expect a defect in inductive capacity of the collecting ducts, or a poor capacity of mesenchyme to be induced, to result in insufficient recruitment of nephrogenic mesenchyme and a persistent peripheral population of

primitive mesenchyme. Analysis of a ureteric bud cell line supernatant with inductive capacity has identified Tgfβ2 as a component of the inducer (Plisov et al., 2001). Considering the many functions that TGFβs display in the control of cell-matrix interactions and the deposition of extracellular matrix (Verrecchia et al., 2001), it is tempting to speculate that the phenotype seen in *Bmp7*$^{cre/+}$*;Smad4*$^{-/CA}$ mutant kidneys is due to an inability of mesenchyme to respond to a TGFβ signal that determines a change in extracellular matrix composition allowing aggregation or compaction of these cells.

In conclusion, the data presented here provide the first evidence that a TGFβ superfamily signal mediated through Smad4 is required to recruit mesenchyme cells from a primitive state in which they display both nephrogenic and stromal characteristics into the nephrogenic mesenchyme. The surprising finding that deletion of *Smad4* in the ureteric bud and collecting ducts does not result in an appreciable phenotype is most readily explained by alternative pathway activation by TGFβ superfamily ligands and receptors, possibly through β-catenin and the Wnt pathway. Further genetic lineage analysis of the early metanephros will clarify our understanding of the sequence of events leading from specification of the metanephric blastema to the segregation of the various cell-types required for morphogenesis.

The authors thank Dr Peter ten Dijke for phospho-Smad1 and phospho-Smad2 antisera, Dr Ray Dunn for critical reading of the manuscript, and Elizabeth Bikoff for insightful comments on the work. L.O. was supported by a fellowship from the Charles A. King Trust and G.C.C. by a fellowship from the Howard Hughes Medical Institute. This work was supported by grants from the NIH to E.J.R.

References

Bard, J. B., Gordon, A., Sharp, L. and Sellers, W. I. (2001). Early nephron formation in the developing mouse kidney. *J. Anat.* **199**, 385-392.

Barnes, J. D., Crosby, J. L., Jones, C. M., Wright, C. V. and Hogan, B. L. (1994). Embryonic expression of Lim-1, the mouse homolog of Xenopus Xlim-1, suggests a role in lateral mesoderm differentiation and neurogenesis. *Dev. Biol.* **161**, 168-178.

Batourina, E., Gim, S., Bello, N., Shy, M., Clagett-Dame, M., Srinivas, S., Costantini, F. and Mendelsohn, C. (2001). Vitamin A controls epithelial/mesenchymal interactions through ret expression. *Nat. Genet.* **27**, 74-78.

Bosukonda, D., Shih, M. S., Sampath, K. T. and Vukicevic, S. (2000). Characterization of receptors for osteogenic protein-1/bone morphogenetic protein-7 (OP-1/BMP-7) in rat kidneys. *Kidney Int.* **58**, 1902-1911.

Bush, K. T., Sakurai, H., Steer, D. L., Leonard, M. O., Sampogna, R. V., Meyer, T. N., Schwesinger, C., Qiao, J. and Nigam, S. K. (2004). TGF-[beta] superfamily members modulate growth, branching, shaping, and patterning of the ureteric bud. *Dev. Biol.* **266**, 285-298.

Chu, G. C., Dunn, N. R., Anderson, D. C., Oxburgh, L. and Robertson, E. J. (2004). Differential requirement for Smad4 in TGFb-dependent patterning of the early mouse embryo. *Development* **131**, 3501-3512.

Clark, A. T., Young, R. J. and Bertram, J. F. (2001). In vitro studies on the roles of transforming growth factor-beta 1 in rat metanephric development. *Kidney Int.* **59**, 1641-1653.

Davies, J. A. and Garrod, D. R. (1995). Induction of early stages of kidney tubule differentiation by lithium ions. *Dev. Biol.* **167**, 50-60.

Dressler, G. R., Deutsch, U., Chowdhury, K., Nornes, H. O. and Gruss, P. (1990). Pax2, a new murine paired-box-containing gene and its expression in the developing excretory system. *Development* **109**, 787-795.

Dudley, A. T. and Robertson, E. J. (1997). Overlapping expression domains of bone morphogenetic protein family members potentially account for limited tissue defects in *BMP7* deficient embryos. *Dev. Dyn.* **208**, 349-362.

Dudley, A. T., Lyons, K. M. and Robertson, E. J. (1995). A requirement for bone morphogenetic protein-7 during development of the mammalian kidney and eye. *Genes Dev.* **9**, 2795-2807.

Dudley, A. T., Godin, R. E. and Robertson, E. J. (1999). Interaction between FGF and BMP signaling pathways regulates development of metanephric mesenchyme. *Genes Dev.* **13**, 1601-1613.

Dymecki, S. M. (1996). Flp recombinase promotes site-specific DNA recombination in embryonic stem cells and transgenic mice. *Proc. Natl. Acad. Sci. USA* **93**, 6191-6196.

Esquela, A. F. and Lee, S. E.-J. (2003). Regulation of metanephric kidney development by growth/differentiation factor 11. *Dev. Biol.* **257**, 356-370.

Godin, R. E., Takaesu, N. T., Robertson, E. J. and Dudley, A. T. (1998). Regulation of BMP7 expression during kidney development. *Development* **125**, 3473-3482.

Gu, H., Zou, Y. R. and Rajewsky, K. (1993). Independent control of immunoglobulin switch recombination at individual switch regions evidenced through Cre-loxP-mediated gene targeting. *Cell* **73**, 1155-1164.

Hellmich, H. L., Kos, L., Cho, E. S., Mahon, K. A. and Zimmer, A. (1996). Embryonic expression of glial cell-line derived neurotrophic factor (GDNF) suggests multiple developmental roles in neural differentiation and epithelial-mesenchymal interactions. *Mech. Dev.* **54**, 95-105.

Herzlinger, D., Abramson, R. and Cohen, D. (1993). Phenotypic conversions in renal development. *J. Cell Sci.* **17**, 61-64.

Hogan, B. L., Beddington, R. S., Costantini, F. and Lacy, E. (1994). *Manipulating the Mouse Embryo: A Laboratory Manual*. Cold Spring Harbor, NY: Cold Spring Harbor Laboratory Press.

Hu, M. C., Piscione, T. D. and Rosenblum, N. D. (2003). Elevated SMAD1/{beta}-catenin molecular complexes and renal medullary cystic dysplasia in ALK3 transgenic mice. *Development* **130**, 2753-2766.

Kreidberg, J. A., Sariola, H., Loring, J. M., Maeda, M., Pelletier, J., Housman, D. and Jaenisch, R. (1993). WT-1 is required for early kidney development. *Cell* **74**, 679-691.

Lagna, G., Hata, A., Hemmati-Brivanlou, A. and Massagué, J. (1996). Partnership between DPC4 and SMAD proteins in TGF-beta signalling pathways. *Nature* **383**, 832-836.

Massagué, J. (2000). How cells read TGF-beta signals. *Nat. Rev. Mol. Cell Biol.* **1**, 169-178.

Mendelsohn, C., Batourina, E., Fung, S., Gilbert, T. and Dodd, J. (1999). Stromal cells mediate retinoid-dependent functions essential for renal development. *Development* **126**, 1139-1148.

Michael, S. K., Brennan, J. and Robertson, E. J. (1999). Efficient gene-specific expression of cre recombinase in the mouse embryo by targeted insertion of a novel IRES-Cre cassette into endogenous loci. *Mech. Dev.* **85**, 35-47.

Miyazaki, Y., Oshima, K., Fogo, A., Hogan, B. L. and Ichikawa, I. (2000). Bone morphogenetic protein 4 regulates the budding site and elongation of the mouse ureter. *J. Clin. Invest.* **105**, 863-873.

Miyazaki, Y., Oshima, K., Fogo, A. and Ichikawa, I. (2003). Evidence that bone morphogenetic protein 4 has multiple biological functions during kidney and urinary tract development. *Kidney Int.* **63**, 835-844.

Miyazono, K., Kusanagi, K. and Inoue, H. (2001). Divergence and convergence of TGF-beta/BMP signaling. *J. Cell Physiol.* **187**, 265-276.

Oxburgh, L. and Robertson, E. J. (2002). Dynamic regulation of Smad expression during mesenchyme to epithelium transition in the metanephric kidney. *Mech. Dev.* **112**, 207-211.

Pachnis, V., Mankoo, B. and Costantini, F. (1993). Expression of the c-ret proto-oncogene during mouse embryogenesis. *Development* **119**, 1005-1017.

Pelton, R. W., Saxena, B., Jones, M., Moses, H. L. and Gold, L. I. (1991). Immunohistochemical localization of TGF beta 1, TGF beta 2, and TGF beta 3 in the mouse embryo: expression patterns suggest multiple roles during embryonic development. *J. Cell Biol.* **115**, 1091-1105.

Persson, U., Izumi, H., Souchelnytskyi, S., Itoh, S., Grimsby, S., Engstrom, U., Heldin, C. H., Funa, K. and ten Dijke, P. (1998). The L45 loop in type I receptors for TGF-beta family members is a critical determinant in specifying Smad isoform activation. *FEBS Lett.* **434**, 83-87.

Piscione, T. D., Yager, T. D., Gupta, I. R., Grinfeld, B., Pei, Y., Attisano, L., Wrana, J. L. and Rosenblum, N. D. (1997). BMP-2 and OP-1 exert direct and opposite effects on renal branching morphogenesis. *Am. J. Physiol.* **273**, F961-F975.

Plisov, S. Y., Yoshino, K., Dove, L. F., Higinbotham, K. G., Rubin, J. S. and Perantoni, A. O. (2001). TGFβ2, LIF and FGF2 cooperate to induce nephrogenesis. *Development* **128**, 1045-1057.

Ritvos, O., Tuuri, T., Eramaa, M., Sainio, K., Hilden, K., Saxen, L. and Gilbert, S. F. (1995). Activin disrupts epithelial branching morphogenesis in developing glandular organs of the mouse. *Mech. Dev.* **50**, 229-245.

Rogers, S. A., Ryan, G., Purchio, A. F. and Hammerman, M. R. (1993). Metanephric transforming growth factor-beta 1 regulates nephrogenesis in vitro. *Am. J. Physiol.* **264**, F996-F1002.

Sanchez, M. P., Silos-Santiago, I., Frisen, J., He, B., Lira, S. A. and Barbacid, M. (1996). Renal agenesis and the absence of enteric neurons in mice lacking GDNF. *Nature* **382**, 70-73.

Sanford, L. P., Ormsby, I., Gittenberger-de Groot, A. C., Sariola, H., Friedman, R., Boivin, G. P., Cardell, E. L. and Doetschman, T. (1997). TGFbeta2 knockout mice have multiple developmental defects that are non-overlapping with other TGFbeta knockout phenotypes. *Development* **124**, 2659-2670.

Saxén, L. (1987). *Organogenesis of the kidney*. Cambridge, UK: Cambridge University Press.

Schnabel, C. A., Selleri, L., Jacobs, Y., Warnke, R. and Cleary, M. L. (2001). Expression of Pbx1b during mammalian organogenesis. *Mech. Dev.* **100**, 131-135.

Schuchardt, A., D'Agati, V., Larsson-Blomberg, L., Costantini, F. and Pachnis, V. (1994). Defects in the kidney and enteric nervous system of mice lacking the tyrosine kinase receptor Ret. *Nature* **367**, 380-383.

Soriano, P. (1999). Generalized lacZ expression with the ROSA26 Cre reporter strain. *Nat. Genet.* **21**, 70-71.

Srinivas, S., Goldberg, M. R., Watanabe, T., D'Agati, V., al-Awqati, Q. and Costantini, F. (1999). Expression of green fluorescent protein in the ureteric bud of transgenic mice: a new tool for the analysis of ureteric bud morphogenesis. *Dev. Genet.* **24**, 241-251.

Vega, Q. C., Worby, C. A., Lechner, M. S., Dixon, J. E. and Dressler, G. R. (1996). Glial cell line-derived neurotrophic factor activates the receptor tyrosine kinase RET and promotes kidney morphogenesis. *Proc. Natl. Acad. Sci. USA* **93**, 10657-10661.

Verrecchia, F., Chu, M. L. and Mauviel, A. (2001). Identification of novel TGF-beta /Smad gene targets in dermal fibroblasts using a combined cDNA microarray/promoter transactivation approach. *J. Biol. Chem.* **276**, 17058-17062.

Vukicevic, S., Latin, V., Chen, P., Batorsky, R., Reddi, A. H. and Sampath, T. K. (1994). Localization of osteogenic protein-1 (bone morphogenetic protein-7) during human embryonic development: high affinity binding to basement membranes. *Biochem. Biophys. Res. Commun.* **198**, 693-700.

Wilkinson, D. G. (1992). *Whole-mount in situ hybridization of vertebrate embryos*. Oxford, UK: IRL Press.

Xiao, Z., Latek, R. and Lodish, H. F. (2003). An extended bipartite nuclear localization signal in Smad4 is required for its nuclear import and transcriptional activity. *Oncogene* **22**, 1057-1069.